

Capillary torque in a liquid bridge between two angled filaments

Amol Bedarkar and Xiang-Fa Wu^{a)}

Department of Mechanical Engineering and Applied Mechanics, North Dakota State University, Fargo, North Dakota 58108-6050, USA

(Received 22 August 2009; accepted 27 October 2009; published online 10 December 2009)

Capillary torque is induced when a liquid bridge forms between two angle-positioned filaments. This paper aims to study the dependency of such capillary torque upon the filament orientation angle, filament spacing, contact angle, and liquid volume through detailed numerical simulation using a surface finite element scheme. Numerical results show that for hydrophilic liquid with contact angle below 90° and at given liquid volume as well as filament spacing, the surface energy of the system grows nonlinearly with increasing filament orientation angle from 0° (parallel filaments) to 90° (cross-positioned filaments). Accordingly, the capillary torque induced by the distorted liquid bridge increases from a torque-free state at 0° to the peak value and then decreases to the second torque-free state at 90° . At fixed filament orientation angle, the capillary torque grows with the liquid volume while decreases rapidly with increasing either contact angle or filament spacing. The peak value of capillary torque depends upon both the geometries and wetting property of the liquid bridge-filament system. A family of characteristic curves in terms of capillary torque with the filament orientation angle is determined at varying volume of liquid bridge, filament spacing ratio, and contact angle. The results and concepts developed in work are applicable for the study of wetting and spreading of liquids in fiber networks, microfluidics-based microstructural assembly, biological cell operation, etc. © 2009 American Institute of Physics.

[doi:[10.1063/1.3267150](https://doi.org/10.1063/1.3267150)]

I. INTRODUCTION

Wetting and spreading of liquids on filaments is of critical importance to a variety of applications, e.g., textile dyeing and cleaning, fiber composite processing, hair caring, etc.^{1–7} For a liquid droplet of sufficient volume sitting symmetrically on a cylindrical filament of circular cross section, it assumes a barrel-shaped morphology, corresponding to an equilibrium state of minimizing the potential energy of the droplet-filament system.^{8,9} The explicit solution of such a droplet-filament wetting problem was first obtained by Carroll,⁸ and has been generalized for developing measurement techniques in characterizing the wetting properties of liquids on filaments.^{10–12} Besides, recent studies have further indicated that two favorable morphologies of droplets could assume on single filaments, i.e., the barrel-shaped⁸ and clamshell-shaped droplets.^{13,14} In reality, the visible morphology of a droplet on filament accords to the lower potential energy of the droplet-filament system.^{13–15} To date, the critical condition of morphology transition from barrel shape to clamshell shape assumed by a droplet on a filament has been determined by McHale *et al.*¹³ using a surface finite element method (SFEM).¹⁶ Similar morphology transition has been also detected in the case of droplets suspended on a pair of parallel filaments, where the morphology transition may happen between a droplet-bridge partially enwrapping the filaments and a barrel-shaped droplet which completely enwraps the filaments in accordance with the principle of minimum potential energy. By means of the SFEM,¹⁶ a family of wetting characteristic curves of droplet-filament rail

systems has been demonstrated recently,¹⁷ in which variation in the critical droplet volume with respect to the filament spacing and contact angle has been justified. Such critical condition needs to be examined before study of droplet spreading in parallel filaments though the latter had started four decades ago based on an asymptotic approach by Princen.¹⁸ Therefore, further studies are still desired in order to refine these approaches.

Furthermore, it is commonly observed that liquid bridge forms between angle-positioned filaments in nature and engineering such as wetting of a spider web by dew and welding of microelectronic components. Among these, when a pair of microfilaments is positioned in an angle and bridged through a liquid droplet, capillary torque will be triggered as a result of the breakage of symmetry of the droplet bridge. Such capillary torque might be responsible for the alignment of wet rodlike particles deposited in drying solutions and the distortion of fiber networks in sensor grids and textiles. To the best of authors' knowledge, no quantitative study has been reported yet on the capillary torque induced by a liquid bridge in the literature.

Thus, in this study, by means of the SFEM,¹⁶ detailed numerical simulations will be performed in determining the capillary torque of a distorted liquid bridge spanned between angle-positioned filaments of identical diameter and surface wetting property. The capillary torque is determined by numerical differentiation of the potential energy of the liquid bridge-filament system with respect to the filament orientation angle. A family of characteristic curves in terms of dimensionless capillary torque versus filament orientation angle will be obtained at varying filament spacing, volume of liquid bridge, and contact angle, which can be regarded as a

^{a)}Electronic mail: xiangfa.wu@ndsu.edu.

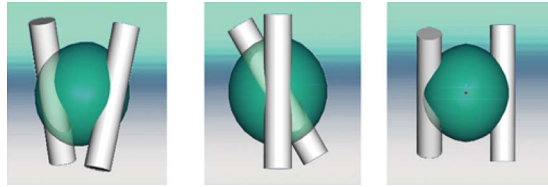


FIG. 1. (Color online) Schematic of a liquid bridge forms between two misaligned filaments of identical diameter and surface wetting properties (filament orientation angle: $\varphi=30^\circ$).

universal law to govern the capillary torque of liquid bridge formed between neighboring filaments. Applications and conclusions of the study will be addressed in the end of the paper.

II. PROBLEM FORMULATION AND NUMERICAL SIMULATIONS

For a liquid bridge formed between two neighboring filaments of identical diameter and surface wetting properties as illustrated in Fig. 1, scaling analysis¹⁹ indicates that the total surface energy of the droplet-filament system can be expressed as

$$\Pi / [(4\pi r^2)\gamma_{LV}] = f[V/(4/3\pi r^3), D/r, \theta, \varphi], \quad (1)$$

where Π (N.m) is the total surface energy of the system, γ_{LV} (N/m) the surface tension of the liquid droplet (liquid-vapor interfacial tension), D (m) the filament spacing (i.e., the minimum distance between the two filament surfaces under consideration), r (m) the radius of the cylindrical filaments of circular cross section, θ the contact angle between the liquid and filament surface, φ the orientation angle between two filaments, and f is a dimensionless function with respect to the dimensionless variables $V/[4/3\pi r^3]$, D/r , θ , and φ . Without loss of generality, dimensionless expression has been adopted in Eq. (1), where r , $4\pi r^2$, and $4/3\pi r^3$ are the reference length, area, and volume, respectively, and the effect of gravity is ignored as considered thereafter for liquid bridges formed by microdroplets.

The capillary torque T triggered by a liquid bridge can be determined by differentiating Eq. (1) with respect to the filament orientation angle φ (radians)

$$\frac{T}{(4\pi r^2)\gamma_{LV}} = \frac{d\Pi/d\varphi}{(4\pi r^2)\gamma_{LV}} = \frac{df[V/(4/3\pi r^3), D/r, \theta, \varphi]}{d\varphi}. \quad (2)$$

Since liquid forms symmetrical bridges between two filaments at $\varphi=0^\circ$ and 90° , there are no capillary torques to be triggered by the liquid bridges at these two limiting angles. Furthermore, in view of physics, the actual morphology of a liquid bridge is the one to minimize the total surface energy of the liquid bridge-filament system. Due to the complex morphology of the liquid bridges under investigation, it is extremely difficult to determine the explicit solution to the resulting Young–Laplace equation at the given boundary conditions even in the simplest cases of $\varphi=0^\circ$ and 90° . Alternatively, recently available SFEM software packages (e.g., SURFACE EVOLVER,¹⁶) provide an efficient, universal numerical tool to determine the surface morphology along with the potential energy of liquid bridges formed in general cases.

In the present study, the SURFACE EVOLVER package¹⁶ is adopted to calculate the surface energies of an arbitrary liquid bridge formed between angle-positioned filaments at varying orientation angle. The yielded surface energies are used to determine the capillary torques induced by the distorted liquid bridge using a numerical differentiation scheme based on Eq. (2). During the numerical process, the filament radius r is fixed as reference length, and surface tension of the droplet γ_{LV} is selected as unit. Two contact angles ($\theta=30^\circ$ and 60°), two filament spacing ratios ($D/r=0.5$ and 1), and two droplet volumes ($V=2$ and 5) are selected, respectively, to explore their influences on the capillary torque. At each case of $(\theta, D/r, V)$, the surface energies of the liquid bridge at 16 filament orientation angles: $\varphi=10^\circ \pm 0.25^\circ$, $20^\circ \pm 0.25^\circ$, $30^\circ \pm 0.25^\circ$, $40^\circ \pm 0.25^\circ$, $50^\circ \pm 0.25^\circ$, $60^\circ \pm 0.25^\circ$, $70^\circ \pm 0.25^\circ$, and $80^\circ \pm 0.25^\circ$ are calculated, respectively. Then, the corresponding capillary torques are determined using an approximate central difference scheme

$$\frac{T|_{\varphi=\varphi_0}}{(4\pi r^2)\gamma_{LV}} = \frac{\Pi[V/(4/3\pi r^3), D/r, \varphi_0 + \Delta\varphi] - \Pi[V/(4/3\pi r^3), D/r, \varphi_0 - \Delta\varphi]}{(4\pi r^2)\gamma_{LV}(2\Delta\varphi)}, \quad (3)$$

where $\Delta\varphi=0.25^\circ=1.3889 \times 10^{-3}\pi$ (radians) is the incremental angular step used in the calculation.

As a matter of fact, numerical solution of the SURFACE EVOLVER is obtained through numerical iteration which has very low convergence rate at fine meshes. It is also found that the surface energy of the liquid bridge-filament system varies very slowly with the change in φ . Thus, in each simulation case, special care has been tested when meshing the liquid bridge in order to accelerate the convergence rate and simultaneously maintain the numerical stability. A simulation process is terminated when the relative numerical errors of

the droplet surface energy are below 1%. Besides, at each φ , at least three numerical simulations have been implemented, and the surface energy with the lowest value is retained for exacting the capillary torque. Finally, all the surface energies of the liquid bridges are determined with respect to varying φ at given D/r , $V/(4/3\pi r^3)$, and θ . After the dimensionless variables are determined on the basis of reference length r , reference area $4\pi r^2$, reference volume $4/3\pi r^3$, and reference energy $4\pi r^2\gamma$, numerical differentiation Eq. (3) is fulfilled and the variation in the dimensionless capillary torque $T/(4\pi r^2\gamma)$ versus the filament orientation angle φ at given

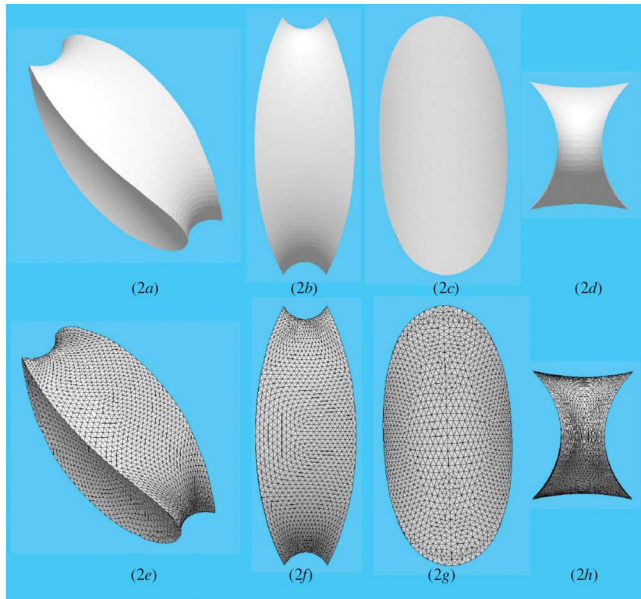


FIG. 2. (Color online) Liquid bridge forms between two parallel filaments of identical diameter and surface wetting properties. (a) 3D view, (b) top view, [(c) and (d)] side views, and [(a)–(h)] corresponding SFEM meshes. [Filaments were not plotted, the simulation was based on SURFACE EVOLVER (Ref. 16) with filament radius $r=1$, filament spacing $D=0.5$, droplet volume $V=2$, and contact angle $\theta=30^\circ$.]

$V/(4/3\pi r)$, D/r and θ can be determined. Detailed results and discussions are made in Sec. III.

III. RESULTS AND DISCUSSIONS

By means of the above approach, Figs. 2–4 demonstrate the surface morphologies of liquid bridge at three different filament orientation angles 0° , 45° , and 90° , respectively, at fixed contact angle 30° , unit filament radius, filament spacing 0.5, and liquid volume 2. These figures indicate that the liq-

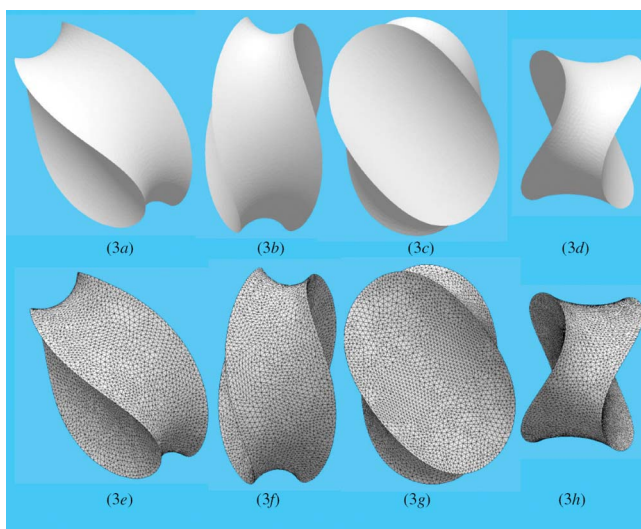


FIG. 3. (Color online) Liquid bridge forms between two misaligned filaments of identical diameter and surface wetting properties (filament orientation angle $\varphi=45^\circ$). (a) 3D view, (b) top view, [(c) and (d)] side views, and [(e)–(h)] corresponding SFEM meshes. [Filaments were not plotted, the simulation was based on SURFACE EVOLVER (Ref. 16) with filament radius $r=1$, filament spacing $D=0.5$, droplet volume $V=2$, and contact angle $\theta=30^\circ$.]

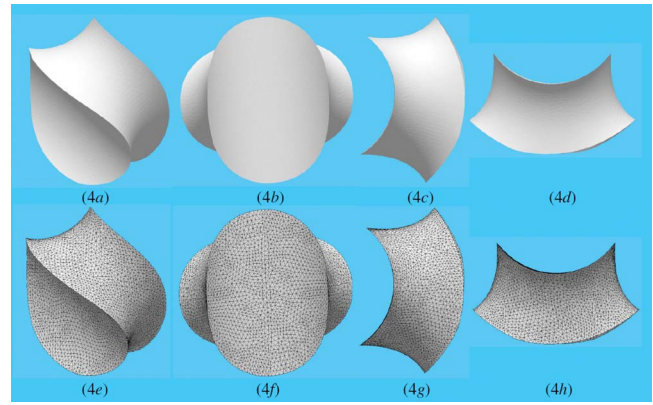


FIG. 4. (Color online) Liquid bridge forms between two cross-positioned filaments of identical diameter and surface wetting properties (filament orientation angle $\varphi=90^\circ$). (a) 3D view, (b) top view, [(c) and (d)] side views, and [(e)–(h)] corresponding SFEM meshes. [Filaments were not plotted, the simulation was based on SURFACE EVOLVER (Ref. 16) with filament radius $r=1$, filament spacing $D=0.5$, droplet volume $V=2$, and contact angle $\theta=30^\circ$.]

uid bridge was distorted gradually with the increase in filament orientation angle φ . Correspondingly, wetting length of the liquid bridge along filament axes shortens with increasing φ ; surface energy of the liquid bridge-filament system grows gradually due to the hydrophilic property of the filament surface in the cases considered in this study. As an example, Fig. 5 shows the typical variation in surface energy of a liquid bridge with φ in the case of $V/(4/3\pi r^3)=0.4775$, $D/r=0.5$ and $\theta=30^\circ$. It can be observed that the surface energy rises nonlinearly with increasing φ .

By using the central difference scheme as given in Eq. (3), a family of characteristic curves is plotted in Fig. 6 in terms of the capillary torques with respect to φ at eight cases of $[D/r, V/(4/3\pi r), \theta]$. In each case, numerical surface energies of the liquid bridge are first obtained at several discrete φ values similar to these plotted in Fig. 5, and then the corresponding capillary torques are extracted, respectively, by the central difference [Eq. (3)]. From Fig. 6, it can be observed that for a hydrophilic liquid under consideration

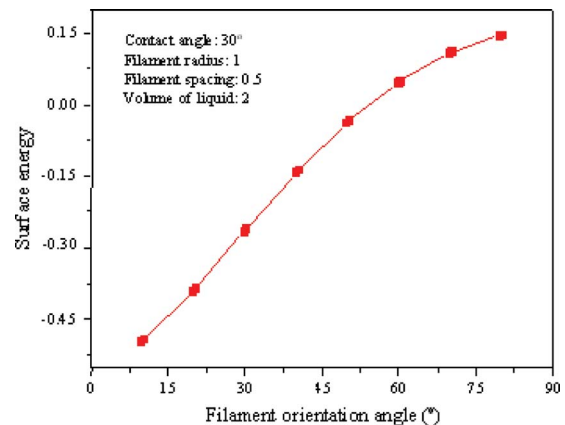


FIG. 5. (Color online) Variation in the surface energy Π vs the filament orientation angle φ of a liquid bridge formed between two filaments of identical diameter and surface wetting properties. [The simulation was based on SURFACE EVOLVER (Ref. 16) with filament radius $r=1$, filament spacing $D=0.5$, droplet volume $V=2$, and contact angle $\theta=30^\circ$.]

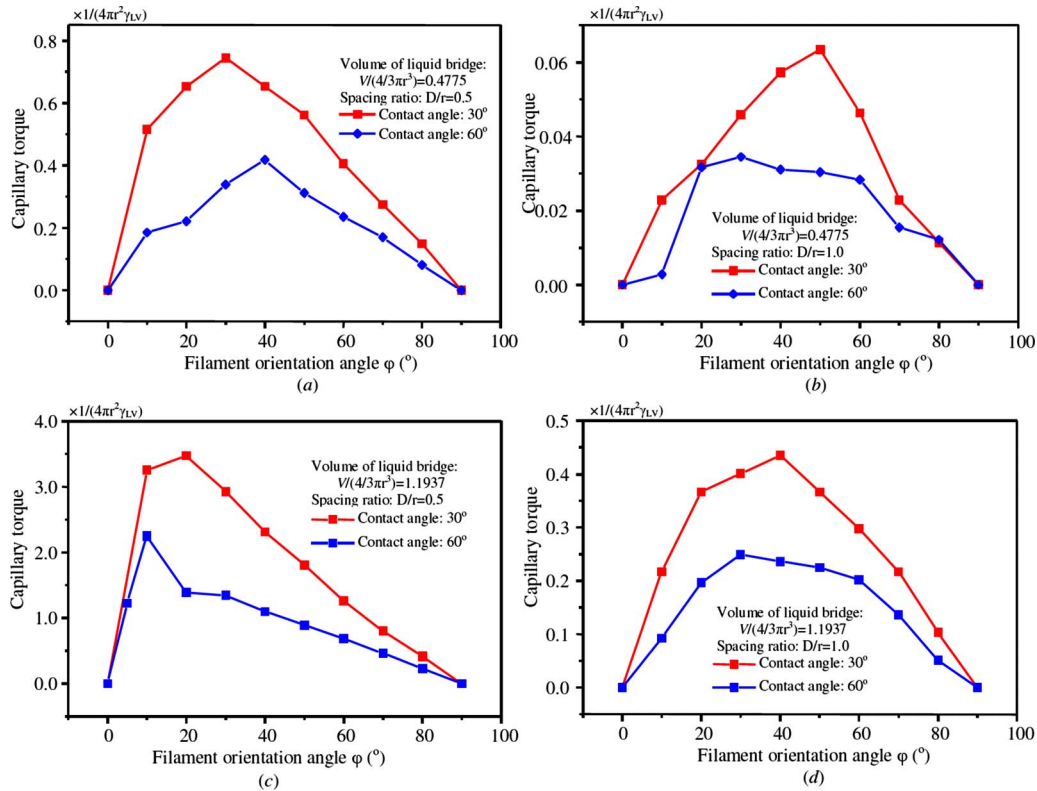


FIG. 6. (Color online) Variation in the dimensionless capillary torque $T/(4\pi r^2 \gamma_{LV})$ vs the filament orientation angle ϕ . (a) Droplet volume $V/(4/3\pi r^3) = 0.4775$, filament spacing $D/r = 0.5$, and contact angles $\theta = 30^\circ$ and 60° , (b) droplet volume $V/(4/3\pi r^3) = 0.4775$, filament spacing $D/r = 1$, and contact angles $\theta = 30^\circ$ and 60° , (c) droplet volume $V/(4/3\pi r^3) = 1.1937$, filament spacing $D/r = 0.5$, and contact angles $\theta = 30^\circ$ and 60° , (d) droplet volume $V/(4/3\pi r^3) = 1.1937$, filament spacing $D/r = 1$, and contact angles $\theta = 30^\circ$ and 60° [Filaments were not plotted, the simulation was based on SURFACE EVOLVER (Ref. 16) with filament radius: $r = 1$.]

(e.g., $\theta = 30^\circ$ and 60°), the capillary torque maintains positive in the range of $\phi \in [0^\circ, 90^\circ]$. Accordingly, the surface energy of liquid bridge increases nonlinearly with increasing ϕ from parallel filament rails ($\phi = 0^\circ$) to a cross-positioned filament pair ($\phi = 90^\circ$). The capillary torque shown in Fig. 6 increases from a torque-free state of two parallel filament rails ($\phi = 0^\circ$) to the peak value and then decreases to a second torque-free state of a pair of cross-positioned filaments ($\phi = 90^\circ$). At fixed filament orientation angle ϕ and filament radius r , the capillary torque grows rapidly with increasing volume of liquid bridge V while decreases with the increase in contact angle θ (i.e., hydrophobicity) and filament spacing. Furthermore, numerical simulations are further executed in the cases of hydrophobic liquids ($\theta > 90^\circ$), however numerical results are unable to converge to stable liquid bridges. As a conclusion, the present simulations indicate that hydrophobic liquid bridge could not be formed between angle-positioned filament pair.

In addition, in typical engineering practice and life experience, the contact angle between liquids and solids is typically below 90° . Thus, stable liquid bridge can form between neighboring misaligned filaments. As a result, capillary torque is triggered due to the nonsymmetrical configuration of the liquid bridge. Such capillary torque could be responsible for the alignment of rodlike particles and microfilaments when they sediment in solutions owing to solvent evaporation in the drying process as commonly observed. Also, such capillary torque can be exploited for the assembly

of microelectronic parts as demonstrated recently,⁷ and other potential applications such as translation and alignment of biological cells, among others.

IV. CONCLUDING REMARKS

In this study, detailed numerical simulations have been performed for determining the morphology, surface energy, and capillary torque of hydrophilic liquid bridge formed between misaligned filaments. A family of characteristic curves in terms of capillary torque versus filament orientation angle has been extracted at varying contact angle, filament spacing, and liquid volume, which gives a quantitative dependency of the capillary torque upon the geometries and wetting properties of the microliquid bridge-filament system. The current numerical experiments also indicate that for hydrophilic liquids, the formed liquid bridges are stable, while it tends to be intrinsically unable in the case of hydrophobic liquid bridges though there is no explicit theoretical reasoning reported yet in the literature which might be responsible for such an observation. Furthermore, the present study has provided a quantitative interpretation of some interesting microfluidic phenomena observed in nature and engineering practice, which could lead to further advanced studies and cutting-edge applications in relevant applied sciences and technologies.

ACKNOWLEDGMENTS

Partial support of this work by the Ashland Aqualon Functional Ingredients Inc., Wilmington, DE and a research initiative grant from NDSU is gratefully acknowledged.

¹P. G. de Gennes, *Rev. Mod. Phys.* **57**, 827 (1985).

²P. G. de Gennes, F. Brochard-Wyart, and D. Quéré, *Capillarity and Wetting Phenomena-Drops, Bubbles, Pearls, Waves* (Springer, New York, 2004).

³V. M. Starov, E. M. Yeatman, M. G. Velarde, and C. J. Radke, *Wetting and Spreading Dynamics* (CRC, Boca Raton, 2007).

⁴D. Bonn, J. Eggers, J. Indekeu, J. Meunier, and E. Rolley, *Rev. Mod. Phys.* **81**, 739 (2009).

⁵D. Quéré, *Annu. Rev. Mater. Res.* **38**, 71 (2008).

⁶D. Lukas and N. Pan, *Polym. Compos.* **24**, 314 (2003).

⁷R. R. A. Syms, V. M. Bright, and G. M. Whitesides, *J. Microelectromech. Syst.* **12**, 387 (2003).

⁸B. J. Carroll, *J. Colloid Interface Sci.* **57**, 488 (1976).

⁹X. F. Wu and Y. A. Dzenis, *Acta Mech.* **185**, 215 (2006).

¹⁰H. D. Wagner, *J. Appl. Phys.* **67**, 1352 (1990).

¹¹B. H. Song, A. Bismarck, R. Tahhan, and J. Springer, *J. Colloid Interface Sci.* **197**, 68 (1998).

¹²N. R. Demarquette, *Int. Mater. Rev.* **48**, 247 (2003).

¹³G. McHale, M. I. Newton, and B. J. Carroll, *Oil Gas Sci. Technol.* **56**, 47 (2001).

¹⁴G. McHale and M. I. Newton, *Colloids Surf., A* **206**, 79 (2002).

¹⁵B. J. Carroll, *Langmuir* **2**, 248 (1986).

¹⁶www.susqu.edu/facstaff/b/vrajjer/evolver

¹⁷X. F. Wu, A. Bedarkar, and K. A. Vaynberg, *J. Colloid Interface Sci.* **341**, 326 (2010).

¹⁸H. M. Princen, *J. Colloid Interface Sci.* **34**, 171 (1970).

¹⁹J. D. Logan, *Applied Mathematics*, 2nd ed. (Wiley, New York, 1996).